

$E0$ decay of the first excited 0^+ states in ^{34}S and ^{38}Ar

K. H. Souw, J. C. Adloff, D. Disdier, and P. Chevallier

Centre de Recherches Nucléaires, Université Louis Pasteur, Strasbourg, France

(Received 24 April 1975)

The reactions $^{31}\text{P}(\alpha, p)^{34}\text{S}$ and $^{35}\text{Cl}(\alpha, p)^{38}\text{Ar}$ have been used to study the $E0$ π decays of the $^{34}\text{S}(3.91 \text{ MeV}, 0^+)$ and $^{38}\text{Ar}(3.38 \text{ MeV}, 0^+)$ states to the ground state. The $E0$ branching ratios Γ_π/Γ were measured to be $(0.38 \pm 0.06) \times 10^{-3}$ and $(6.6 \pm 1.0) \times 10^{-3}$, respectively. When these values are combined with the available lifetime of these states, $E0$ matrix elements $\langle M \rangle_\pi = (1.55 \pm 0.15) \text{ fm}^2$ (^{34}S) and $(2.26 \pm 0.21) \text{ fm}^2$ (^{38}Ar) are obtained.

NUCLEAR REACTIONS $^{31}\text{P}(\alpha, p)$, $E = 7.60 \text{ MeV}$; $^{35}\text{Cl}(\alpha, p)$, $E = 7.67 \text{ MeV}$; ^{34}S , ^{38}Ar measured $E0$ branching ratios. Deduced $E0$ matrix elements. Natural targets.

I. INTRODUCTION

In the $2s-1d$ shell the structures of the first excited 0^+ states in even-even nuclei are generally not well known. In the simple harmonic oscillator approximation, the ground state (g.s.) $E0$ decays of these states disappear. Nonvanishing $E0$ decays can be predicted if more sophisticated potentials, such as Woods-Saxon, are used in the calculations, or if p shell or $f-p$ shell excitations are taken into account. $E0$ decay measurements on such states provide direct tests of the importance of these excitations in the structure of the states and of the behavior of the radial wave functions in the vicinity of the nucleus surface.

Recently, $E0$ decay measurements relevant to the first excited 0^+ states in $(4n+2)$ nuclei of the $2s-1d$ shell have been reported in ^{18}O (Ref. 1), ^{26}Mg (Refs. 2 and 3), and ^{30}Si (Refs. 3 and 4). They show that the $E0$ strength strongly diminishes from 1.8 single particle units (s.p.u.) (^{18}O) to 0.052 s.p.u. (^{30}Si). Small $E0$ strengths were also observed for $^{32}\text{S}(0.11 \text{ s.p.u.})^5$ and $^{36}\text{S}(0.038 \text{ s.p.u.})^6$. In order to check if there is some systematic behavior in the $E0$ decays of the first excited 0^+ states across the $2s-1d$ shell in $(4n+2)$ nuclei, we measured the g.s. π -branching ratio (BR) of the $^{34}\text{S}(3.91 \text{ MeV}, 0^+)$ and $^{38}\text{Ar}(3.38 \text{ MeV}, 0^+)$ states. The experimental method described in Ref. 3 was used.

II. EXPERIMENTAL RESULTS

The reactions $^{31}\text{P}(\alpha, p)^{34}\text{S}$ at $E_\alpha = 7.60 \text{ MeV}$ and $^{35}\text{Cl}(\alpha, p)^{38}\text{Ar}$ at $E_\alpha = 7.67 \text{ MeV}$ were used to populate the 3.91-MeV state in ^{34}S and the 3.38-MeV state in ^{38}Ar . The $^4\text{He}^{++}$ beams were delivered by the 5.5-MV Van de Graaff accelerator of the Centre de Recherches Nucléaires. The phosphorus targets of $\approx 200 \mu\text{g}/\text{cm}^2$ on $250\text{-}\mu\text{g}/\text{cm}^2$ gold backings were prepared following the method given in Ref. 7. The natural BaCl_2 targets of $300 \mu\text{g}/\text{cm}^2$

were evaporated onto $250\text{-}\mu\text{g}/\text{cm}^2$ gold backings. The protons were detected in a $150\text{-mm}^2\text{-}300\text{-}\mu\text{m}$ -thick surface barrier annular counter. The surface of this detector was covered by a $50\text{-}\mu\text{m}$ aluminum foil in the ^{34}S run and by a $70\text{-}\mu\text{m}$ one in the ^{38}Ar run. These absorbers ensured that only protons were detected. Plastic scintillator telescopes with 0.2- or 0.4-mm thick ΔE counters³ were used for the π detection.

A. $^{34}\text{S}(3.91 \text{ MeV}, 0^+)(\pi)^{34}\text{S}(\text{g.s.})$ decay

The results of a 30-h measurement taken with a 70-nA beam current and the 0.2-mm-thick ΔE counters in the telescopes are represented in Figs. 1 and 2(a). Figure 1(a) is the direct singles proton spectrum from the $^{31}\text{P}(\alpha, p)^{34}\text{S}$ reaction. Figure 1(b) is the projection onto the proton energy axis of the two-dimensional proton energy versus π -energy spectrum (not represented) taken simultaneously with the spectrum of Fig. 1(a). Figure 2(a) displays the projection onto the π -energy axis of the two-dimensional spectrum in proton channels 32-37. In subtracting the γ - γ contribution from the 3.91-MeV γ -ray cascade via the 2.13-MeV state, the procedure given in Ref. 5 was used. We found 177 ± 27 pairs from the 3.91-MeV state to g.s. π decay, which when combined with the 3.91-MeV proton yield in channels 32-37 of Fig. 1(a) and the calculated π efficiency,³ give $\Gamma_\pi/\Gamma = (3.9 \pm 0.8) \times 10^{-4}$ for the 3.91-MeV state.

The use of telescopes with 0.4-mm-thick ΔE counters produces a more favorable ratio of number of detected pairs to number of detected γ - γ interactions.³ In order to get a better π spectrum for the 3.91-MeV decay, we made a measurement with these telescopes. The resulting π spectrum is shown Fig. 2(b). From this measurement we deduce $\Gamma_\pi/\Gamma = (3.8 \pm 0.6) \times 10^{-4}$ for the 3.91-MeV state.

We take $\Gamma_\pi/\Gamma = (3.8 \pm 0.6) \times 10^{-4}$, the mean weighted value from the two runs, as our result. When

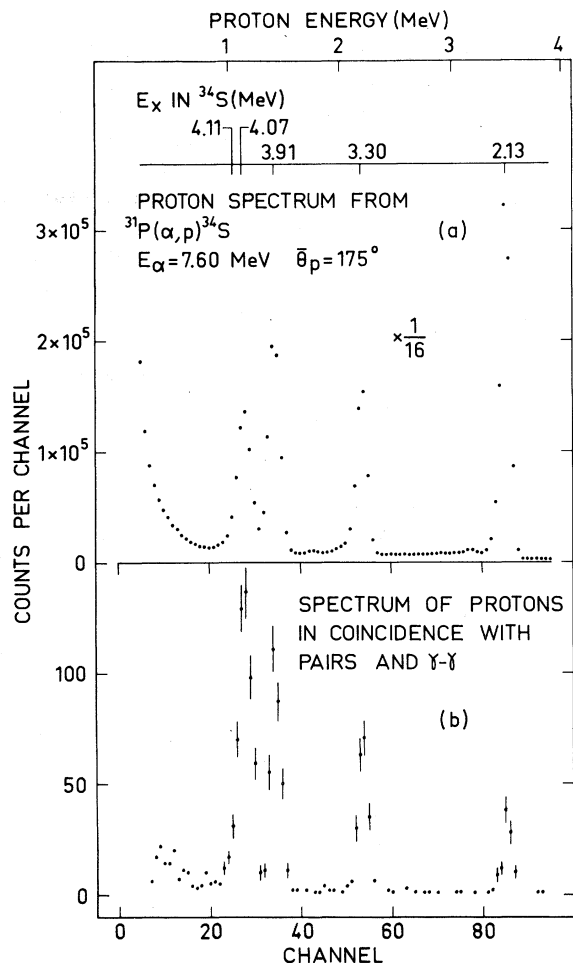


FIG. 1. (a) $\frac{1}{16}$ sampled direct proton spectrum from $^{31}\text{P}(\alpha, p)^{34}\text{S}$ taken simultaneously with the nonrepresented proton energy vs π -energy spectrum. (b) Projection onto the proton energy axis of the two-dimensional proton energy vs π -energy spectrum.

combined with $\tau_m = (1.60 \pm 0.13)$ psec,⁹ the partial π lifetime of the 3.91-MeV state in ^{34}S is found to be $\tau_\pi = (4.2 \pm 0.8)$ nsec. The value of the monopole matrix element deduced from this value of τ_π is $\langle M \rangle_\pi = (1.55 \pm 0.15) \text{ fm}^2$.

B. $^{38}\text{Ar}(3.38 \text{ MeV}, 0^+) (\pi)^{38}\text{Ar}(\text{g.s.})$ decay

In Fig. 3 are represented the results of a 12-h measurement with a 180-nA beam current. This figure is for ^{38}Ar and its meaning is the same as that of Fig. 2 in Sec. II A. By following the same procedure as in Sec. II A we deduced a value $\Gamma_\pi / \Gamma = (6.6 \pm 1.0) \times 10^{-3}$ for the 3.38 MeV to g.s. π decay in ^{38}Ar . When this value is combined with $\tau_m = (29 \pm 3)$ psec,⁹ the partial π lifetimes of the 3.38-MeV state is $\tau_\pi = (4.4 \pm 0.8)$ nsec. The value of the $E0$ matrix element deduced from the value of τ_π is $\langle M \rangle_\pi = (2.26 \pm 0.21) \text{ fm}^2$.

III. DISCUSSION

In Table I we show a comparison of $E0$ decays relevant to the first excited 0^+ states in $(4n+2)$ nuclei of the p , s - d , and f - p shells. The s.p.u. strength of these decays is plotted as a function

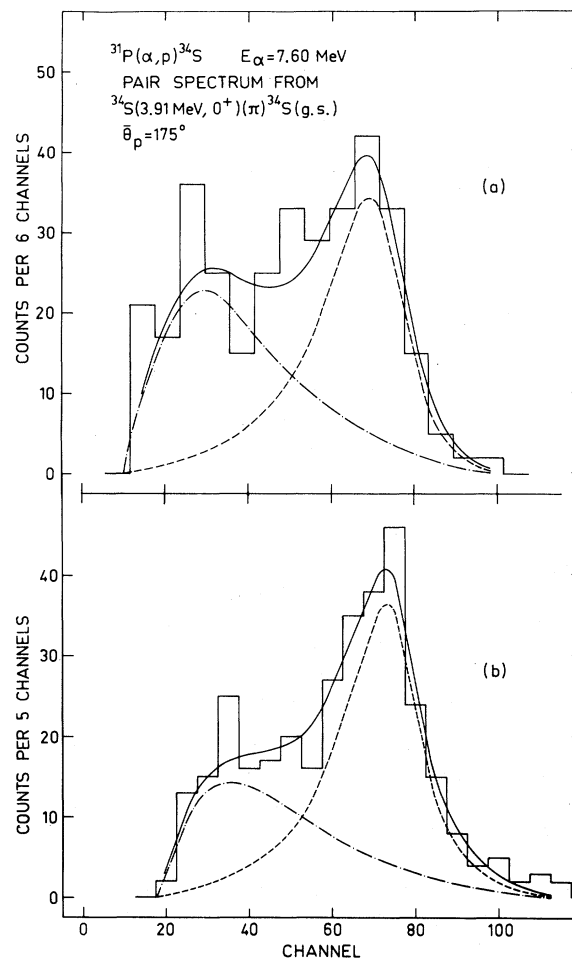


FIG. 2. (a) Pair spectrum obtained from the projection of events in channels 32-37 of Fig. 1(b) onto the π -energy axis of the relevant proton energy vs π -energy spectrum. The dashed-dotted line is the shape of the γ - γ interactions in the telescopes due to the 3.91 MeV \rightarrow 2.13 MeV \rightarrow g.s. γ -ray cascade. The dashed line is the shape of the π spectrum from the 3.91 MeV \rightarrow g.s. π decay. The weighting of these two curves was obtained by a least squares fit. The number of γ - γ interactions is in good agreement with that calculated by using $(1.5 \pm 0.3) \times 10^{-5}$ γ - γ interactions per detected proton (Refs. 3 and 5). (b) Pair spectrum for the 3.91 MeV \rightarrow g.s. π decay obtained by using the telescopes mounted with 0.4-mm-thick ΔE plastic counters (Ref. 3). The significance of the dashed-dotted and dashed curves is the same as in part (a). The number of γ - γ interactions is in good agreement with that calculated by using $(2.3 \pm 0.5) \times 10^{-5}$ γ - γ interactions per detected proton (Ref. 3).

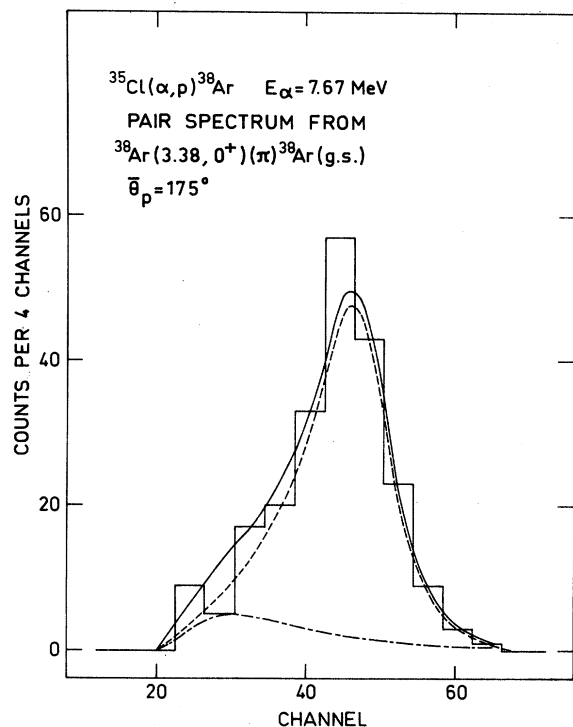


FIG. 3. Pair spectrum from the decay of the $^{38}\text{Ar}(3.38 \text{ MeV}, 0^+)$ state to g.s. in coincidence with the protons from the $^{35}\text{Cl}(\alpha, p)^{38}\text{Ar}$ reaction. The dashed-dotted line is the shape of the γ - γ interactions in the telescopes due to the $3.38 \text{ MeV} \rightarrow 2.17 \text{ MeV} \rightarrow \text{g.s.}$ γ -ray cascade. The dashed line is the shape of the π spectrum from the $3.38 \text{ MeV} \rightarrow \text{g.s.}$ π decay.

of the mass number in Fig. 4. In this figure, a systematic behavior of the strength across the shell clearly appears. One notices that the greatest strengths occur around the closed ^{16}O and ^{40}Ca shells for ^{16}O and ^{42}Ca . In the middle of the s - d shell the $E0$ strengths are quite small, and become smaller yet in the f - p shell (^{58}Ni). The values of the $E0$ strength from the first excited 0^+ state to g.s. in ^{16}O (0.74 s.p.u.) and ^{40}Ca (0.13 s.p.u.) are indicated in Fig. 4 by the arrows.

It is interesting to remark that the known $E0$ decays in the sulphur isotopes likewise exhibit small strengths. These values are presented in Table II.

In Fig. 4 are also plotted the $E2$ transition strengths in Weisskopf units for the γ decays from the first excited 0^+ state to the first excited 2^+ state in some $(4n+2)$ nuclei. In calculating these strengths the lifetimes given in Table I were used together with the γ -BR given in Ref. 9. As can be seen from the figure, there is some analogy in the behavior of the $E2$ and $E0$ strengths across the shells. This behavior might be due to some systematic correlation in the wave functions of the involved g.s. and first excited 2^+ states.

In the s - d shell, with the exception of ^{18}O recently discussed in Ref. 1, there are no predictions available for values of $E0$ matrix elements. The excitation energies of the low-lying states in $(4n+2)$ nuclei of the shell from magnesium to sulphur are generally quite reasonably reproduced if only $1d_{5/2}$, $2s_{1/2}$, and $1d_{3/2}$ configurations are taken into account in the calculations, as in Refs. 29-34. However, the predicted $B(E2)$ values for the $E2$ γ -ray decay of the first excited 0^+ state to the first excited 2^+ state are usually at

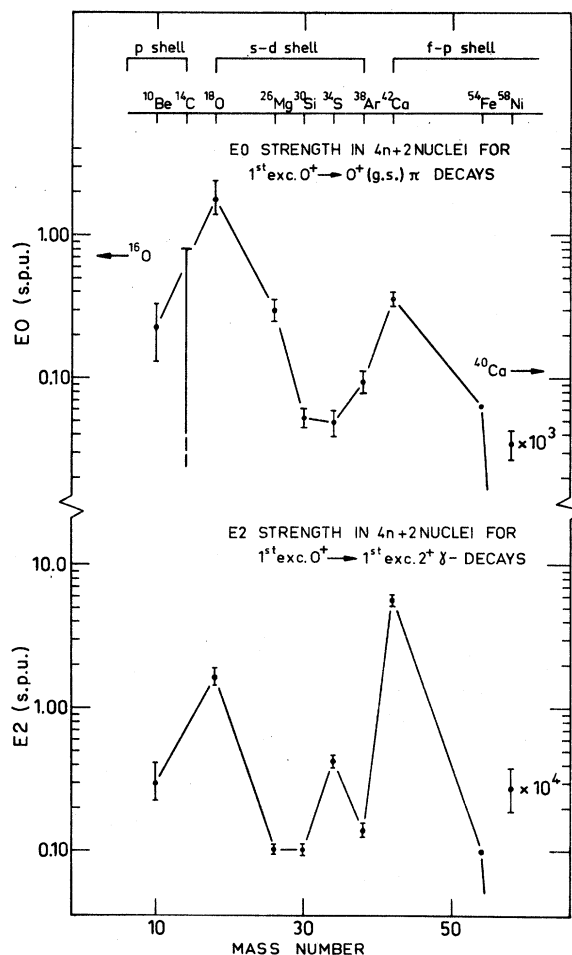


FIG. 4. $E0$ and $E2$ single particle unit strengths in $(4n+2)$ nuclei as a function of the mass number for the first excited 0^+ to g.s. π decay (upper part of the figure) and for the first excited 0^+ to first excited 2^+ state decay (lower part). In the case of ^{58}Ni these strengths are off scale and so are represented, respectively, in the figure multiplied by 10^3 and 10^4 . The strengths in the case of ^{54}Fe are obtained by taking the single particle estimate for the lifetime of the first excited 0^+ state in ^{54}Fe (see Ref. 21). The $E0$ strength for ^{14}C is an upper limit of ≤ 0.81 s.p.u. (see Ref. 11). The values of the $E0$ strengths of the 6.05- and 3.35-MeV states in ^{16}O (0.74 s.p.u.) and ^{40}Ca (0.13 s.p.u.) are indicated by the arrows.

TABLE I. Properties of $J^\pi=0^+$ excited states in $(4n+2)$ nuclei for $A \leq 58$.

Nucleus	E_x (MeV)	τ_m (psec)	Ref.	Γ_π/Γ ($\times 10^{-3}$) ^a	Ref.	$\langle M \rangle_\pi$ (fm ²) ^a	Ref.	$E0$ strength ^b (s.p.u.)
¹⁰ Be	6.18	$1.1^{+0.4}_{-0.3}$	10	2.4 ± 0.8	10	$1.45^{+0.63}_{-0.72}$	10	$0.23^{+0.10}_{-0.11}$
¹⁴ C	6.59	>0.6	11	10 ± 4	11	<3.39	11	<0.81
¹⁸ O	3.63	1.39 ± 0.16 ^c	12, 13	3.0 ± 0.6	1	6.0 ± 0.7	1	1.8 ± 0.4
	5.33	0.20 ± 0.04	13	≤ 2.3	1	≤ 4.5	1	≤ 1
²⁶ Mg	3.59	9.5 ± 0.6 ^d	14, 15	5.1 ± 0.7	3	3.00 ± 0.25	3	0.29 ± 0.05
	4.97	$0.70^{+0.15}_{-0.10}$ ^e	16, 17	...		4.23 ± 0.46	(e, e')2	0.55 ± 0.12
	6.22	$0.06^{+0.05}_{-0.04}$	16	...		3.33 ± 0.20	(e, e')2	0.34 ± 0.04
³⁰ Si	3.79	15.6 ± 1.2	15	2.7 ± 0.4	4	1.46 ± 0.12	4	$(5.4 \pm 0.9) \times 10^{-2}$
				2.6 ± 0.6	3	1.4 ± 0.2	3	$(5.2 \pm 1.3) \times 10^{-2}$
³⁴ S	3.91	1.60 ± 0.13	8	0.38 ± 0.06	This work	1.55 ± 0.15	This work	$(5.2 \pm 1.0) \times 10^{-2}$
³⁸ Ar	3.38	29 ± 3	9	6.6 ± 1.0	This work	2.26 ± 0.21	This work	$(9.5 \pm 1.8) \times 10^{-2}$
⁴² Ca	1.84	480 ± 30	18	...		7.13 ± 0.70	23	0.82 ± 0.16
						4.70 ± 0.26	24	0.36 ± 0.04
⁵⁴ Fe	2.56	>2.02	19	1.70 ± 0.25	21	<8.8		<0.9
⁵⁸ Ni	2.94	$(2.9 \pm 0.1) \times 10^3$	20	0.22 ± 0.05	22	$(5.8 \pm 0.6) \times 10^{-2}$	22	$(3.5 \pm 0.8) \times 10^{-5}$

^a For ground-state decays.^b See Ref. 25.^c Mean weighted values deduced from Refs. 12 and 13.^d Mean weighted values deduced from Refs. 14 and 15.^e Mean weighted values deduced from Refs. 16 and 17.

least 2 times smaller than the observed ones. Monopole matrix elements in the case of a pure s - d description for the initial and final 0^+ states vanish if harmonic oscillator radial wave functions are used. This property arises from the orthogonality of the wave functions and from the fact that for harmonic oscillator radial wave functions, the mean square radius $\langle r^2 \rangle$ is the same for all the subshells of the s - d shell. Different values for $\langle r^2 \rangle$ for the subshells, and hence nonvanishing $E0$ matrix elements, are obtained if Woods-Saxon radial wave functions were used. Thus the finite matrix elements reported for s - d shell nuclei in Tables I and II would arise from a radial wave function behavior which is different from that of a harmonic oscillator one.

It has been shown that near the closed shells, for ¹⁸O and ³⁸Ar, deformed 0^+ intruder states due to core excitations can appear in the level scheme

in the vicinity of the first pure s - d 0^+ excited state. In fact there are reasons to believe that in ¹⁸O (see Ref. 1) and ³⁸Ar (Refs. 35 and 36), the first excited 0^+ state is itself such an intruder state. Core excitation configurations might be present in the first excited 0^+ states of the other s - d shell nuclei since they have nonvanishing $E0$ matrix elements (Tables I and II). The behavior of the $E0$ strengths in the $(4n+2)$ nuclei of the s - d shell could therefore also be due to a change in the amount of core excitation configuration mixing in the low-lying 0^+ states across the shell. Still this does not exclude the importance of knowing the exact nature of the radial wave function.

Let us focus more attention on ³⁸Ar. A calculation of Gray *et al.*³⁶ has shown that the first deformed 0^+ state occurs in ³⁸Ar at ≈ 3.8 MeV with 81% of an $(f_{7/2})^2(d_{3/2})^{-4} 2p4h$ configuration. The small predicted spectroscopic factor of 0.03 for

TABLE II. Properties of the first excited $J^\pi=0^+$ states of sulphur isotopes.

Nucleus	E_x (MeV)	τ_m (psec)	Ref.	$\langle M \rangle_\pi$ (fm ²)	Ref.	$E0$ strength ^a (s.p.u.)
³² S	3.78	0.90 ± 0.15	9	2.22 ± 0.27	5	$(11.0 \pm 3.0) \times 10^{-2}$
				1.95 ± 0.5	(e, e') 26, 27	
³⁴ S	3.91	1.60 ± 0.13	8	1.55 ± 0.15	This work	$(5.2 \pm 1.0) \times 10^{-2}$
³⁶ S	3.35	$(1.27 \pm 0.03) \times 10^4$	6	1.38 ± 0.03	6, 28	$(3.8 \pm 0.1) \times 10^{-2}$

^a See Ref. 25.

this level in the ³⁹K(*d*, ³He)³⁸Ar reaction is not in strong disagreement with the measured upper limit of 0.01 for the ³⁸Ar(3.38 MeV, 0⁺) state.³⁶ However, the *B*(*E*2) value of (11.3 ± 1.2) *e*² fm⁴, deduced from τ_{*m*} = (29 ± 3) psec⁹ for the 3.38–2.17 MeV *E*2 γ-ray decay, is poorly reproduced in their calculations which yield *B*(*E*2) = 0.9 *e*² fm⁴ with an effective proton and neutron charge of 1.0. The enhanced *E*0 strength for the 3.38-MeV to g.s. π decay with respect to the middle of the *s*-*d* shell observed in our work may indicate a larger contribution of core excited configurations in the structure of the 0⁺ states. For these reasons, the first excited 0⁺ state in ³⁸Ar, as in ¹⁸O, might be a core excited state. It is interesting to mention that the second excited 0⁺ state in ³⁸Ar was found at 4.71 MeV.⁹ A nearly pure *s*-*d* state is predicted at that energy by Gray *et al.*³⁶ which could be identified as the pure first excited 0⁺ *s*-*d* state predicted by Wildenthal *et al.*³⁴ A similar situation might exist in ⁴²Ca (Refs. 37–39) where 0⁺ states are observed at 1.84 MeV, 5.60 MeV, and possibly at 3.30 MeV (Ref. 9).

One has to point out that in all *s*-*d* shell nuclei reported in Fig. 4, a second excited 0⁺ state is observed near 5 MeV excitation. *E*0 decay measurements for these higher states would be a good way to shed more light on the structure of the lower-lying 0⁺ states in the *s*-*d* shell.

Within the isospin formalism the monopole operator $\sum_p r_p^2$ is written $\frac{1}{2}\sum_i r_i^2 - \frac{1}{2}\sum_i \tau_3^{(i)} r_i^2$, containing an isoscalar and an isovector part, and where the sums are taken over all nucleons with the τ₃^(*i*) operator eigenvalues +1 corresponding to neutrons and -1 to the protons. By considering only the isoscalar part, the monopole energy-weighted isoscalar sum rule⁴⁰ for *T* = 1 → *T* = 1

transitions is

$$\sum_n \hbar\omega_n \left| \langle n | \frac{1}{2} \sum_i r_i^2 | 0 \rangle \right|^2 = \frac{A\hbar^2}{2m} R_m^2,$$

where *R*_{*m*}² is the mean square matter radius averaged over the *A* nucleons of the g.s. |0⟩ and *m* the nucleon mass. The *E*0 decays reported in Table I exhaust the following percentages of this sum rule: ¹⁸O(3.63 MeV) ≈ 5%, ²⁶Mg(3.58 MeV) ≈ 0.7%, ³⁰Si(3.79 MeV) ≈ 0.1%, ³⁴S(3.91 MeV) ≈ 0.1%, ³⁸Ar(3.38 MeV) ≈ 0.2%, and ⁴²Ca(1.84 MeV) ≈ 0.4%. In calculating these percentages, identical matter and charge mean square radii *R*_{*m*}² = *R*_{*c*}² = *r*₀² *A*^{2/3} were assumed with *r*₀ = 1.03 fm as deduced from muonic x-rays and electron scattering experiments for 17 ≤ *A* ≤ 40. The very small contribution to the isoscalar sum rule for (4*n* + 2) nuclei with *A* > 18 has to be emphasized. A strong contribution of an isovector part in a measured *E*0 matrix element, which however is unlikely, could render even smaller the preceding percentages. As a matter of fact, that the isovector contribution in the complete energy-weighted sum rule for *T* → *T*, *T*₃ ≠ 0 *E*0 transitions is small might be deduced by analogy with electric γ-ray transition sum rules (see Ref. 41). Nevertheless, it would be interesting to get an estimate of the isovector contribution in *E*0 matrix elements of low-lying 0⁺ states in (4*n* + 2) nuclei. Such contributions could be obtained by measuring the analog *E*0 decays in *T*₃ = -1 nuclei and by comparing these results with those available in *T*₃ = +1 nuclei, providing *T* = 2 isospin impurities are small in low-lying 0⁺ states.

We would like to thank Dr. A. Pape for critically reading the manuscript and Miss M. A. Saettel for preparing the ³¹P targets.

¹K. H. Souw, J. C. Adloff, D. Disdier, and P. Chevallier, Phys. Rev. C **11**, 1899 (1975).
²E. W. Lees, A. Johnston, S. W. Brain, C. S. Curran, W. A. Gillespie, and R. P. Singhal, J. Phys. A **7**, 936 (1974).
³J. C. Adloff, K. H. Souw, D. Disdier, F. Scheibling, P. Chevallier, and Y. Wolfson, Phys. Rev. C **10**, 1819 (1974).
⁴E. K. Warburton and D. E. Alburger, Phys. Rev. C **10**, 1570 (1974).
⁵J. C. Adloff, K. H. Souw, D. Disdier, and P. Chevallier, Phys. Rev. C **11**, 738 (1975).
⁶J. W. Olness, W. R. Harris, A. Gallmann, F. Jundt, D. E. Alburger, and D. H. Wilkinson, Phys. Rev. C **3**, 2323 (1971).
⁷B. W. Hooton, Nucl. Instrum. Methods **27**, 338 (1964).
⁸M. W. Greene, P. R. Alderson, D. C. Bailey, J. L. Durell, L. L. Green, A. N. James, and J. F. Sharpey-Schafer, Nucl. Phys. **A148**, 351 (1970).

⁹P. M. Endt and C. Van der Leun, Nucl. Phys. **A214**, 1 (1973).
¹⁰D. E. Alburger, E. K. Warburton, A. Gallmann, and D. H. Wilkinson, Phys. Rev. **185**, 1242 (1969).
¹¹D. E. Alburger, A. Gallmann, J. B. Nelson, J. T. Sample, and E. K. Warburton, Phys. Rev. **148**, 1050 (1966).
¹²E. K. Warburton, P. Gorodetzky, and J. A. Becker, Phys. Rev. C **8**, 418 (1973).
¹³J. W. Olness, E. K. Warburton, and J. A. Becker, Phys. Rev. C **7**, 2239 (1973).
¹⁴Z. Berant, C. Broude, G. Engler, and M. J. Renan, Nucl. Phys. **A218**, 324 (1974).
¹⁵F. Beck, P. Engelstein, and J. P. Vivien, Nucl. Phys. **A228**, 393 (1974).
¹⁶O. Häusser, T. K. Alexander, and C. Broude, Can. J. Phys. **46**, 1035 (1968).
¹⁷J. L. Durell, P. R. Alderson, D. C. Bailey, L. L. Green, M. W. Greene, A. N. James, and J. F. Sharpey-

- Schafer, J. Phys. A 5, 302 (1972).
- ¹⁸P. C. Simms, N. Benczer-Koller, and C. S. Wu, Phys. Rev. 121, 1169 (1961).
- ¹⁹J. M. Moss, UCRL Report No. UCRL-18902, 1969 (unpublished).
- ²⁰D. F. H. Start, R. Anderson, L. E. Carlson, A. G. Robertson, and M. A. Grace, Nucl. Phys. A162, 49 (1971).
- ²¹E. K. Warburton and D. E. Alburger, Phys. Rev. C 6, 1224 (1972).
- ²²E. K. Warburton and D. E. Alburger, Phys. Lett. 36B, 38 (1971).
- ²³N. Benczer-Koller, M. Nessim, and T. H. Kruse, Phys. Rev. 123, 262 (1961).
- ²⁴B. N. Belyaev, S. S. Vasilenko, and D. M. Kaminker, Izv. Akad. Nauk, SSSR Ser. Fiz. 35, 806 (1971) [Bull. Acad. Sci. USSR Phys. Ser. 35, 742 (1971)].
- ²⁵D. H. Wilkinson, Nucl. Phys. A133, 1 (1969).
- ²⁶P. Strehl, Z. Phys. 234, 416 (1970).
- ²⁷Mainz group, Germany (unpublished).
- ²⁸E. A. Samworth and J. W. Olness, Phys. Rev. C 5, 1238 (1972).
- ²⁹K. W. C. Stewart and B. Castel, Nucl. Phys. A132, 445 (1969).
- ³⁰J. F. A. Van Hienen, P. W. M. Glaudemans, and J. Van Lidth de Jeude, Nucl. Phys. A225, 119 (1974).
- ³¹G. Craig, Nucl. Phys. A225, 493 (1974).
- ³²B. H. Wildenthal, J. B. McGrory, E. C. Halbert, and H. D. Graber, Phys. Rev. C 4, 1708 (1971).
- ³³P. W. M. Glaudemans, P. M. Endt, and A. E. L. Dieperink, Ann. Phys. (N.Y.) 63, 134 (1971).
- ³⁴B. H. Wildenthal, E. C. Halbert, J. B. McGrory, and T. T. S. Kuo, Phys. Rev. C 4, 1266 (1971).
- ³⁵G. A. P. Engelbertink and P. W. M. Glaudemans, Nucl. Phys. A123, 225 (1969).
- ³⁶W. S. Gray, P. J. Ellis, T. Wei, R. M. Polichar, and J. Jänecke, Nucl. Phys. A140, 494 (1970).
- ³⁷G. F. Bertsch, Nucl. Phys. 89, 673 (1966).
- ³⁸W. J. Gerace and A. M. Green, Nucl. Phys. A93, 110 (1967).
- ³⁹B. H. Flowers and L. D. Skouras, Nucl. Phys. A136, 353 (1969).
- ⁴⁰R. A. Ferrell, Phys. Rev. 107, 1631 (1957).
- ⁴¹E. K. Warburton and J. Weneser, in *Isospin in Nuclear Physics*, edited by D. H. Wilkinson (North-Holland, Amsterdam, 1969), p. 173.